Antiviral Research 91 (2011) 267–277

Contents lists available at ScienceDirect

Antiviral Research

journal homepage: www.elsevier.com/locate/antiviral

Inactivation of a non-enveloped RNA virus by artificial ribonucleases: Honey bees and Acute bee paralysis virus as a new experimental model for *in vivo* antiviral activity assessment

Antonina A. Fedorova [a,1], Klara Azzami [b,1], Elena I. Ryabchikova [a], Yulia E. Spitsyna [a], Vladimir N. Silnikov [a], Wolfgang Ritter [c], Hans J. Gross [b], Jürgen Tautz [b], Valentin V. Vlassov [a], Hildburg Beier [b], Marina A. Zenkova [a,*]

[a] *Institute of Chemical Biology and Fundamental Medicine, SB RAS, 630090 Novosibirsk, Russian Federation*
[b] *BEEgroup, Biocenter, University of Würzburg, Am Hubland, D-97074 Würzburg, Germany*
[c] *Department of Bee Pathology, CVUA-Animal Health, D-79108 Freiburg, Germany*

ARTICLE INFO

Article history:
Received 10 December 2010
Revised 3 May 2011
Accepted 16 June 2011
Available online 22 June 2011

Keywords:
Artificial ribonucleases
Virus inactivation
Antiviral activity
Killed-virus vaccine
Acute bee paralysis virus
Bee larvae

ABSTRACT

RNA-containing viruses represent a global threat to the health and wellbeing of humans and animals. Hence, the discovery of new approaches for the design of novel vaccines and antiviral compounds attains high attention. Here we describe the potential of artificial ribonucleases (aRNases), low molecular weight compounds capable to cleave phosphodiester bonds in RNA under mild conditions, to act as antiviral compounds *via* destroying the genome of non-enveloped RNA viruses, and the potential of utilizing honey bee larvae and adult bees (*Apis mellifera*) as a novel experimental system for the screening of new antiviral compounds. Pre-incubation of an Acute bee paralysis virus (ABPV) suspension with aRNases D3–12, K-D-1 or Dp12F6 in a concentration-dependent manner increased the survival rate of bee larvae and adult bees subsequently infected with these preparations, whereas incubation of the virus with aRNases ABL3C3 or L2–3 had no effect at all. The results of RT-PCR analysis of viral RNA isolated from aRNase-treated virus particles confirmed that virus inactivation occurs *via* degradation of viral genomic RNA: dose-dependent inactivation of ABPV correlates well with the cleavage of viral RNA. Electron microscopy analysis revealed that the morphology of ABPV particles inactivated by aRNases remains unaffected as compared to control virus preparations. Altogether the obtained results clearly demonstrate the potential of aRNases as a new virus inactivation agents and bee larvae/ABPV as a new *in vivo* system for the screening of antiviral compounds.

1. Introduction

RNA-containing viruses cause many serious diseases both in mammals (HIV, Influenza virus, Poliomyelitis virus, Foot-and-Mouth disease virus) and insects. The study of virus life cycle, virus assembly and disassembly permits to investigate ways to combat the infection and to develop inhibitors of viral enzymes or vaccines. One strategy employed to inactivate viruses is to degrade or modify the genomic RNA, while leaving the protein coat intact (Singer and Fraenkel-Conrat, 1969). These inactivated virions are potentially vaccines, as all the antigenic determinants of the parent virion remain unaffected.

Genomic RNA modification can be achieved by the penetration of chemical substances through the viral envelope and capsid (Broo et al., 2001; Goncharova et al., 2009). To be effective the chemical must be able to pass through the virion shell as well as to cause RNA inactivation. Hence, the size of the "capsid hole" imposes restrictions on the size of chemical agents expected to act as RNA inactivators. In this respect, chemical compounds such as artificial ribonucleases (aRNases), which are small synthetic organic molecules capable to cleave phosphodiester bonds in RNA in a broad range of conditions, can be considered as potential antiviral agents (Zenkova et al., 2001; Kuznetsova and Silnikov, 2004). In this study, five aRNases of three different series developed in the ICBFM (Novosibirsk, Russia) were studied (Fig. 1). Synthesis and RNA cleaving activity of the aRNases were described previously (Konevets et al., 1999; Zenkova et al., 2001; Kovalev et al., 2008; Tamkovich et al., 2007, 2010). The compounds functionally mimic RNase A and cleave RNA predominantly at Pyr-A phosphodiester

* Corresponding author. Tel.: +7 383 363 51 60; fax: +7 383 363 51 53.
E-mail addresses: marzen@niboch.nsc.ru, fedorova.antonia@gmail.com (M.A. Zenkova).
[1] Both authors have contributed equally to this work.

0166-3542/$ - see front matter © 2011 Elsevier B.V. All rights reserved.
doi:10.1016/j.antiviral.2011.06.011

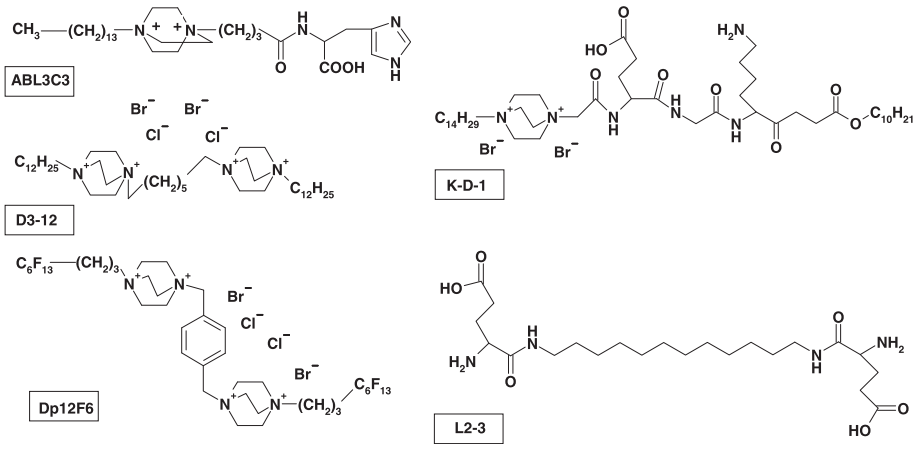

Fig. 1. Structures of artificial ribonucleases (aRNases) used in the study. Designations of the compounds are boxed. The aRNases ABL3C3 and K-D-1 are built of structures that provide affinity to RNA (DABCO: 1.4-diaza-bicyclo[2.2.2]octane residue, bearing two positive charges at quarternized nitrogen atoms) and groups that can catalyze the cleavage of phosphodiester bonds in RNA (histidine in ABL3C3 and lysine and glutamic acid in K-D-1). The aRNases D3–12 and Dp12F6 contain two DABCO moieties as RNA-binding domain, but lack any functionalities which can catalyze transesterification reaction. The aRNase L2–3 is a peptide-like molecule built of two glutamine residues connected by a hydrophobic linker (Konevets et al., 1999; Zenkova et al., 2001; Kovalev et al., 2006, 2008; Tamkovich et al., 2007, 2010).

linkages (5′-C–A-3′ and 5′-U–A-3′) located within single stranded regions of RNA or within regions with a labile secondary structure (Zenkova et al., 2001; Kuznetsova et al., 2005; Tamkovich et al., 2010). These compounds are targeted at RNA and do not react with the protein shell of viral capsids under physiological conditions. Recently, it was shown that some aRNases are able to inactivate enveloped viruses (Influenza A/WSN/33 (H1N1), *Paramixoviridae*) *in vitro*, causing degradation of genomic RNA and introducing local breaks in the lipid membrane of the virus, but leaving the total structure of the virus particle unaltered (Goncharova et al., 2009). The ability of aRNases to inactivate non-enveloped RNA viruses was still uncertain.

RNA-containing Acute bee paralysis virus (ABPV) was used as a model virus to study the effect of aRNases on non-enveloped viruses because: a) the complete genomic sequence is elucidated (Govan et al., 2000), b) physico-chemical properties of the virions are known (Bailey et al., 1963; Newman et al., 1973), and c) the effects of ABPV infection on honey bees was intensively studied (Bailey et al., 1963; Ball, 1985; Genersch and Aubert, 2010). Moreover, purified ABPV suspensions retain the infectivity if stored at −20 °C. This virus was originally considered as a picorna-like virus, but has been recently assigned to the new family *Dicistroviridae* (Genersch and Aubert, 2010). ABPV has a single-stranded positive-sense polyadenylated 9.491 nt long RNA genome (Govan et al., 2000) with two open reading frames (ORFs) separated by an intragenic region. The virions are about 30 nm in diameter. The structure of dicistrovirus capsids shows similarities to vertebrate non-enveloped picornaviruses but with some intriguing differences (Tate et al., 1999).

In this study using a new highly sensitive *in vivo* model based on honey bee larvae (*Apis mellifera*) challenged with ABPV, we demonstrated that aRNases are able to inactivate the non-enveloped RNA virus. Two out of five examined aRNases effectively inactivate ABPV *via* destruction of viral RNA (as shown by RT-PCR analysis), leaving the protein capsid unaltered (as revealed by electron microscopy). These findings underline the potential of aRNases for inactivation of RNA viruses, preparation of killed-virus vaccine and the feasibility of the bee larvae/ABPV experimental model for the antiviral/virucidal activity assessment.

2. Materials and methods

2.1. Oligonucleotides and artificial ribonucleases

The aRNases were synthesized by Dr. D. Konevets and Dr. V. Silnikov (ICBFM, Novosibirsk, Russia) and dissolved in DMSO (Sigma, St. Louis, MO) at concentrations ranging from 20 to 50 mM; further dilutions were performed using MilliQ water (Millipore, Billerica, MA) or appropriate buffer. Purchased oligodeoxyribonucleotide primers were synthesized by phosphoramidite method and purified by HPLC (Biosan, Russia). Sequences of the oligonucleotides are listed in Table 1.

2.2. Cell culture

Multiple drug resistant human cell line KB-8-5 growing in the presence of 300 nM vinblastine was generously provided by Prof. M. Gottesman (NIH, Bethesda, MD). The cells were grown in DMEM supplemented with 10% FBS, 100 units/ml penicillin, 100 μg/ml streptomycin, 0.25 μg/ml amphotericin and 300 nM vinblastine, at 37 °C in a humidified atmosphere containing 5% CO_2.

2.3. Isolation of virus and determination of concentration

As a source of ABPV used in all experiments carried out in this study served a single highly purified virus suspension prepared at the CVUA laboratory (Freiburg, Germany). For virus propagation, an ABPV suspension was injected into the haemocoel of white-eye worker pupae of honey bees (*A. mellifera*). Then the infected pupae were maintained in the incubator at 35 °C for three days and the

Table 1
Oligonucleotide primer pairs selected for the amplification of ABPV and MDR1 RNA fragments by RT-PCR.

	Primer set	Length of product, [bp]	Primer sequence 5′ → 3′	Nucleotide positions
1	ABPV_1_f[a]	516	CCCAACGCACAAACAAATA	567–585
	ABPV_1_r[a]		CTCCAGACAACAACAACAA	1064–1082
2	ABPV_2_f	882	CCCAACGCACAAACAAATA	567–585
	ABPV_2_r		CACACACATCAACCACAC	1431–1448
3	ABPV_3_f	836	TACAAAGCAACCAGCAAG	613–630
	ABPV_3_r		CACACACATCAACCACAC	1431–1448
4	ABPV_4_f[b]	773	TATCAGAAGGCCACTGGAGA	6242–6261
	ABPV_4_r[b]		TCCACTCGGTCATCATAAGG	6995–7014
5	ABPV_5_f[b]	779	TCTTGGACATTGCCTTCAGT	6848–6867
	ABPV_5_r[b]		ATACCATTCGCCACCTTGTT	7607–7626
	MDR1_f[c]	628	GCTGTTCGTTTCCTTTAGGT	46–65
	MDR1_r[c]		ATCATCTGTAAGTCGGGTGTTA	653–674

[a] Letter f and r designate forward and reverse primers, respectively.
[b] Primer sets described by Bakonyi et al. (2002).
[c] Primer set described by Kostenko et al. (2002).

virus was extracted from the species by homogenization and successive centrifugation steps. The concentration and the purity of the virus suspension were determined spectrophotometrically (A_{260} = 5 OD/ml; A_{260}/A_{280} = 1.7). Furthermore, the absence of Sacbrood virus (SBV) and Deformed wing virus (DWV) was confirmed by agar gel immunodiffusion tests. The physical titer of the virus suspension was estimated to be 10^{12} particles/ml by means of electron microscopy using a routine method (Mittereder et al., 1996). The concentration of the virus suspension is further presented in terms of LD_{50}: LD_{50} is the dose of ABPV, which causes death of 50% of the injected larvae after 24 h. In this study 1 LD_{50} corresponds to 1 μl of a 10^{-7}-diluted stock virus suspension (about 10^2 virus particles).

2.4. Virus inactivation

Mixtures of the total volume 50–140 μl containing 100 LD_{50}/μl of ABPV suspension (10^4 particles/μl), 50 mM Tris–HCl, pH 7.0, 200 mM KCl, 0.2 mM EDTA were incubated at 37 °C for 18 h in the presence of one of the examined aRNases at a concentration range of 0.04–400 (Dp12F6), 1–400 μM (D3–12), 0.01–1 (K-D-1), 0.5 (D3), and 1 mM (L2–3). As a control, ABPV suspension was incubated under the same conditions but in the absence of aRNases.

2.5. Origin of honey bee larvae and adults

During the summer seasons 2008–2009, worker honey bee larvae and adult bees were obtained from two colonies with sister queens of *A. mellifera carnica* maintained in the apiary of the BEEstation (University of Wuerzburg, Germany).

2.6. In vitro rearing of worker bee larvae, adult bees collection and toxicity assay

Larvae were collected from a comb with a special grafting tool and transferred to 24-well plates filled with 300 μl of basic diet as previously described (Randolt et al., 2008). The larvae were maintained in an incubator at 35 °C and 80% relative humidity. Each day they were transferred to a new 24-well plate filled with the fresh diet until reaching an average weight of 40–60 mg (4–4.5 days after hatching, fourth instar stage).

Freshly emerged bees were obtained from a caged comb placed in an incubator at 35 °C about 20 days after the deposition of eggs by a queen confined on a comb without brood, divided into groups of 20 individuals and proceeded for antiviral activity assessment.

For injections we used disposable calibrated (1–5 μl) glass capillaries (Servoprax, Hartenstein, Wuerzburg, Germany) with fine tips that were generated by a P-2000 laser-based micropipette puller (Sutter Instruments, Novato, CA).

For the toxicity assay, the larvae were divided into groups, each containing 8–10 individuals, and 1 μl of the aRNase solution in phosphate-buffered saline (PBS) with concentrations ranging from 0.1 to 1 mM for L2–3, from 4 to 400 μM for D3–12, from 4 to 400 μM for Dp12F6 and from 0.1 to 1 mM for K-D-1 was dorsally injected into larvae. As a negative control, larvae injected with PBS and non-injected individuals were used. The toxicity was evaluated 24 h p.i. by (a) the extent of larval survival, (b) phenotype of larvae, and (c) protein expression pattern in the haemolymph. Haemolymph collection was carried out as previously described (Randolt et al., 2008). As stock aRNase solutions (20–50 mM) were prepared in 100% DMSO the inhibitory effect of serial dilutions of DMSO itself was examined by injection into larvae. It was found that ⩽2% DMSO solution in PBS is harmless for larvae. All experiments were run in two replicates. Wilcoxon rank-sum test was used to evaluate the statistical significance of the differences between the groups and to calculate the p value.

2.7. Antiviral activity assessment

An aliquot (1 μl) containing 10 or 100 LD_{50} of ABPV suspension, pre-treated *in vitro* with one of the examined aRNases, was dorsally injected into fourth instar larvae (8–10 larvae per each group). As controls served (a) untreated larvae, (b) larvae mock-infected with PBS, (c) larvae challenged with control virus suspension incubated in the absence of aRNase at 37 °C for 18 h, and d) larvae challenged with the native ABPV.

After collection, newly emerged adults (20 individuals per each group) were chilled on ice and injections of 100 LD_{50} of ABPV (1 μl) either pre-incubated with aRNases (D3–12 or Dp12F6), or control ABPV (pre-incubated in the absence of aRNases) were performed with glass capillaries into the haemocoel laterally between the second and third tergit. As a negative controls, bees injected with PBS and non-injected bees were used. After the injections, bees of each group were kept in small metal boxes supplied with 45% (w/v) sucrose solution in an incubator at 35 °C until haemolymph collection.

The extent of virus inactivation was controlled for bee larvae and adult bees 24 and 48 h p.i., respectively, using three parameters: 1) survival rate, 2) phenotype, and 3) proteomic analysis of the haemolymph originating from the same individuals (Randolt et al., 2008). All experiments were run in triplicate. Wilcoxon rank-sum test was used to evaluate the statistical significance of the differences between the groups and to calculate the p value.

2.8. SDS polyacrylamide gel electrophoresis

Gel electrophoresis was run as described (Randolt et al., 2008). One-dimensional gel electrophoresis was carried out in vertical 10% polyacrylamide gels (8.5 × 13 × 0.1 cm) containing 0.1% SDS with a 1.5-cm-long 5% stacking gel on top of the separating gel (Laemmli, 1970). Haemolymph samples were diluted with 2×concentrated sample buffer (100 mM Tris–HCl, pH 6.8, 4% SDS, 17% glycerol, and 0.8 M 2-mercaptoethanol), heated for 3 min at 95 °C and subjected to electrophoresis at constant voltage (120 V). For colloidal Coomassie staining, the gels were fixed for 30 min in 0.85% *o*-phosphoric acid/20% methanol and then stained overnight in a solution of Roti®-Blue (Roth, Karlsruhe, Germany) in 20% methanol according to the manufacturer's instructions. Gels were destained in 25% methanol.

2.9. RNA extraction

To verify the effective isolation of viral RNA and the absence of RNA loss during the isolation steps and RT-PCR analysis, the total RNA of KB-8-5 cells was used as internal control. KB-8-5 cells are carcinoma cells grown in the presence of 300 nM vinblastine and overexpressing the *MDR1* gene (GenBank accession no. M14758). KB-8-5 cells in the exponential phase of growth were plated on 15 cm^2 culture plates (5 × 10^5 cells/plate), grown until reaching the 80% monolayer, trypsinized, harvested and counted. Total RNA of KB-8-5 cells was extracted using Mammalian Total RNA Kit (Sigma, USA). For the extraction, 9 × 10^6 cells were pelleted for 5 min at 1000 rpm. The culture medium was removed and discarded, the cells were mixed with 500 μl of lysis solution/β-ME mixture and proceeded exactly as described by the manufacturer (http://www.sigmaaldrich.com/). The purity of isolated RNA was confirmed by 1.5% agarose electrophoresis at 5 V/cm^2. Concentration of the extracted RNA was measured spectrophotometrically by the absorbance at 260 nm, the A_{260}/A_{280} ratio did not exceed 1.8.

After the incubation of virus suspension in the presence or in the absence of aRNase the viral RNA was extracted according to the QIAamp Viral RNA extraction Kit protocol. The virus suspension (140 μl) containing 100 LD_{50}/μl (10^4 particles/μl) was added to

560 μl of lysis buffer simultaneously with 1.12 μg of total RNA, isolated from KB-8-5 cells and 5.6 μg of RNA-carrier. Then all procedures were exactly as described by the manufacturer (http://www.qiagen.com/). Obtained RNA samples were used for RT-PCR or stored at −20 °C until analysis.

2.10. Reverse transcription, primer design and PCR

Ten μl of the viral RNA samples were used to prepare cDNA with 100 units of MMLV reverse transcriptase. The RT reaction was carried out for 1 h at 37 °C with hexanucleotide random primers and 1.25 mM of each dNTP in buffer, containing 50 mM Tris–HCl, pH 8.3, 75 mM KCl, 3 mM $MgCl_2$, 5 mM DTT in a total reaction volume of 30 μl. Three pairs of oligonucleotide primers (Table 1) were designed based on the published ABPV genome (GenBank accession no. AF150629) using the Primer Designer program (CLC Main Work Bench 5, Version 5.5). Two primer pairs described by Bakonyi et al. (2002) were used as positive controls of ABPV RNA amplification (Table 1). PCR was performed in 100 mM Tris–HCl, pH 8.3, containing 500 mM KCl, 1.5 mM $MgCl_2$, 0.01% Tween 20, with 2 units of *Taq* DNA polymerase, 0.25 mM of each dNTP, 20 pmol MDR primers (Kostenko et al, 2002) and 30 pmol of one of the ABPV primer set **1–5** using 2 μl of cDNA template. Thermocycler conditions included initial denaturation at 95 °C for 2 min followed by 29–33 cycles consisting of 95 °C for 1 min, 55 °C for 1 min, 72 °C for 1 min. The PCR products were run in 1% agarose gel using 1 × TBE as running buffer and visualized by ethidium bromide staining. All experimental points were run in triplicate.

2.11. Electron microscopy

The morphology of the aRNase Dp12F6, as well as the intact ABPV particles, pre-incubated either with aRNase Dp12F6 or in the absence of aRNase, was examined in negatively stained preparations. To this end, mixtures of the total volume 1 ml containing 10^4 LD_{50}/μl (10^6 particles/μl) were incubated in the presence of 0.4 mM Dp12F6 for 0, 1, 5, 8, 12 and 24 h at 37 °C. Copper grid covered by formvar film was placed for 30 s on a drop (20–30 μl) of virus suspension, then excess of the preparation was removed by filter paper, and grid was placed on a drop of phosphotungstic acid (PTA) for 20 s. The excess of PTA was removed by filter paper, and dried grids were examined in JEM 1400 transmission electron microscope (Jeol, Japan) at 80 kV. Identical treatment was applied for the visualization of the aRNase Dp12F6. Digital images were obtained by the Jeol digital camera and Veleta (SIS) digital camera integrated in Jem 1400 electron microscope.

Concentration of ABPV suspension in the aRNase-treated samples was evaluated using polystyrene latex beads (Sigma) having a diameter of 100 nm with known concentration of 10^{11} particles/ml. Before negative staining control and aRNase-treated virus preparations were 10-fold concentrated with Centricon YM-10 (Amicon Bioseparations, Millipore Corp., Beverly, MA). Virus and latex suspensions were treated by ultrasound for 10 and 30 min, respectively, then equal volumes (15 μl) of the suspensions were mixed and again treated by ultrasound for 10 min. The mixtures were negatively stained and the ABPV concentration was determined according to routine method (Mittereder et al., 1996) after 0, 8 and 24 h of incubation in the presence of Dp12F6.

3. Results

3.1. Validation of larvae as a model for antiviral activity assessment

To confirm the validity of employing a new bee larvae model for the assessment of the antiviral activity of aRNases, we evaluated the toxicity of four (out of five) studied compounds. Experimental groups of 8–10 bee larvae at the fourth instar stage received injections of aRNase solutions in PBS. A group of non-injected larvae was used as a control (n.i.), and to visualize the effect of wounding another group of larvae was mock-infected with PBS. The survival rate 24 h p.i. for each group of larvae challenged with aRNases was in a range from 82% to 100%, which is comparable to the survival rate of mock-infected and non-injected larvae (Table 2). The larvae were classified as dead when they had lost their body elasticity, stopped rhythmical movements and/or displayed colour changes accompanied by growth retardation. The phenotypes of bee larvae challenged with PBS and two different concentrations of aRNase Dp12F6 24 h p.i. shown as an example in Fig. 2A are similar. Dead larvae can be pinpointed in wells b-4 and c-3.

The haemolymph of bee larvae contains a number of prominent proteins that have recently been identified by MS/MS analysis (Randolt et al., 2008). Clearly, the larval-specific protein pattern remains unaltered as compared to PBS-injected and not injected individuals, even after the injection of high doses (400 μM) of the aRNase Dp12F6 (Fig. 2B).

Overall, the low toxicity of the examined aRNases is confirmed by the lack of larval growth retardation, unaltered survival rate and haemolymph protein pattern of bee larvae as compared to non-injected or mock-infected individuals. This is in contrast to the high toxicity of aRNases exerted in MDCK cells. The cell-inhibitory concentration (IC50) is in the range of 8–15 μM for aRNase D3–12 and 40–70 μM for aRNase Dp12F6 (Table 2).

3.2. Antiviral activity of aRNases

The *in vitro* challenge of larvae and adult bees by the injection of a defined amount of bacteria or viruses into the haemocoel allows to study the response of individuals dependent on the employed dose (Randolt et al., 2008). The impact of an ABPV infection on larvae and adult bees differs considerably. Adult bees first develop the typical trembling and signs of paralysis followed by death within 48 h at the critical ABPV dose of 10^4 virus particles per bee. In turn, larvae respond to ABPV infection (10^3 virus particles per bee larvae, 10 LD_{50}) with a much more severe reaction, which resulted in a sudden collapse of all the infected individuals within 20–24 h p.i., accompanied by growth retardation and an extreme colour change of the larvae from yellowish-white to brownish-black. The almost simultaneous response of bee larvae challenged with ABPV, which express a pronounced phenotype, facilitated the study of the effects of aRNases on ABPV inactivation.

We examined each of the five compounds (Fig. 1) for the ability to inactivate ABPV *in vitro*. Therefore, ABPV suspension was pre-incubated *in vitro* with one of the aRNases at a concentration

Table 2
Effects of aRNases on the survival rate of bee larvae.

aRNase	Larvae		Cell culture, IC_{50}, mM[b]
	[aRNase], mM	Survival rate, %[a]	
Dp12F6	0.4	88 ± 2.8[c]	
D3–12	0.4	82 ± 6.4[c]	
K-D-1	1	100[c]	0.08–0.15
L2–3	1	94 ± 4.2[c]	>5
ABL3C3	not determined		0.1–0.5
PBS	–	95 ± 7.1[c]	–
n.i.	–	100	–

[a] Extent of larval survival 24 h post-injection of 1 μl of PBS or of 1 μl of aRNase at the indicated concentration (for details see Section 2.6). The results show the mean ± standard deviation of two independent series of experiments.

[b] IC_{50} – cell-inhibitory concentration refers to the concentration of the compound when 50% of MDCK cells survive (Goncharova, unpublished data).

[c] The statistically insignificant difference $p > 0.05$ between each experimental group and n.i. larvae. *P* values were calculated using the Wilcoxon rank sum test.

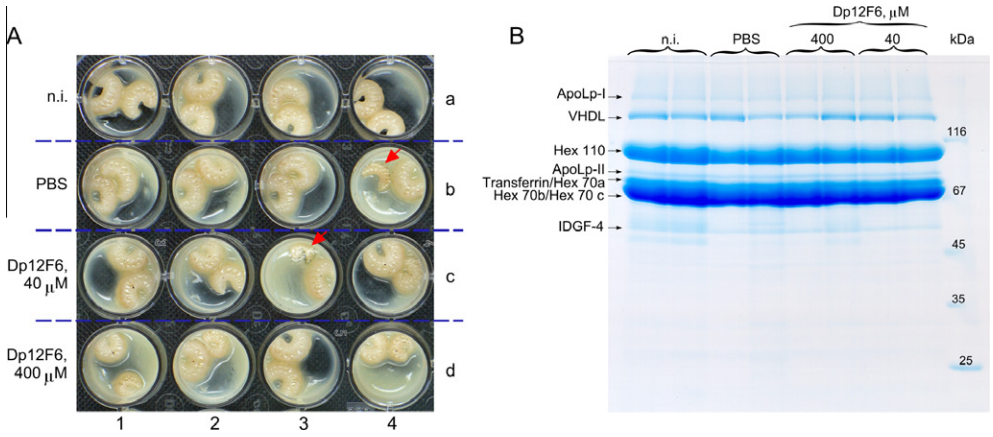

Fig. 2. Development of *in vitro* cultured bee larvae is not impaired after application of aRNase (toxicity test). (A) The phenotype of bee larvae upon 24 h post-injection of two different concentrations of Dp12F6 is shown. The development of non-infected (n.i.) and mock-injected (PBS) larvae is illustrated. Dead larvae are marked by red arrowheads. (B) Protein expression pattern in the haemolymph samples collected from each of two individuals out of the larval groups seen in A (wells a to d). Aliquots of these samples (1 μl) were mixed with dissociation buffer and applied onto a 10% polyacrylamide/0.1% SDS gel.

ranging from 0.04 μM to 1 mM for 18 h at 37 °C and then aliquots of 1 μl, containing 10 LD_{50} (10^3 virus particles) were injected into fourth instar larvae. As controls served non-injected and PBS-injected larvae and larvae injected with ABPV pre-incubated in the absence of aRNase (control ABPV). In the first two control groups 100 and 95 ± 7.1% individuals survived, while the deadly collapse (0% survival rate) of all individuals within 24 h p.i. was observed in the third group (injected with control ABPV).

As summarized in Table 3, two out of five aRNases exhibited a prominent virucidal activity. After pre-incubation of the ABPV suspension with D3–12 (10 μM) or Dp12F6 (4 μM) followed by injections of 10 LD_{50} into larvae 95 ± 4.2 and 89 ± 19% survival of infected individuals, respectively, was observed. After pre-incubation of ABPV in the presence of 0.1 mM and 1 mM of K-D-1, we observed 19 ± 7.8% and 77 ± 25.2%, larval survival, respectively. However, reproducibility of these results was low possibly due to the poor solubility of the aRNase and/or its tendency to form aggregates. The aRNases L2–3 and ABL3C3 had no measurable effects on larval survival upon ABPV infection even at the highest concentration of these compounds (Table 3). Based on the results of this initial screening, we focused our attention on the two most active aRNases D3–12 and Dp12F6 that exhibit a high virucidal activity along with a low toxicity (Tables 2 and 3).

In our next studies in parallel to bee larvae as a model organism we also included young adult bees. For both developmental stages of worker bees, a concentration-dependent profile of the ABPV inactivation by the two aRNases can be seen (Fig. 3). However, the evaluation of the survival rate of non-infected and infected adult bees is hampered, firstly, by a reduced survival rate (80–90%) of non-injected individuals. Secondly, the onset of symptoms after ABPV infection may vary between 24 and 48 h p.i.

Table 3
Antiviral activity of aRNases against ABPV.

aRNase	ABPV inactivation		Ribonuclease activity *in vitro*	
	[aRNase], mM [a]	Larvae survival rate, %[b]	[aRNase], mM[c]	Cleavage extent, %[c]
Dp12F6	0.004	89 ± 19[d]	0.01	60 ± 5
D3–12	0.01	95 ± 4.2[d]	0.01	50 ± 5
K-D-1	1	77 ± 25.2[d]	0.1	95 ± 5
L2–3	1	0[e]	1	95 ± 5
ABL3C3	0.5	0[e]	0.1	80 ± 8
Control ABPV	–	0	–	–
PBS	–	95 ± 7.1	–	–

[a] Concentration of aRNase corresponding to the maximal level of ABPV inactivation, determined in the larval survival assay;

[b] Extent of larval survival 24 h post-injection of 10 LD_{50} of either ABPV treated with aRNase and ABPV treated under the same conditions but in the absence of aRNase (control ABPV). Injection of PBS served as a control for wounding. The results show the mean ± standard deviation of three independent series of experiments.

[c] Concentration of aRNase at which the maximal extent of RNA cleavage was observed *in vitro*. (Konevets et al., 1999; Zenkova et al., 2001; Kovalev et al., 2008). The listed extents of RNA cleavage were observed after incubation of [^{32}P]-labeled RNA with aRNase at 37 °C for 6 h in the case of K-D-1 and L2–3, for 10 °h in the case of D3–12 and Dp12F6 and for 18 h in the case of ABL3C3. RNA cleavage was performed in 50 mM Tris–HCl buffer, pH 7.0 containing 0.2 M KCl, 0.1 mM EDTA supplemented with 100 μg/mL of RNA carrier (for details see Zenkova et al., 2001).

[d] The statistically significant difference ($p < 0.01$) as compared to control ABPV. p values were calculated using the Wilcoxon rank sum test.

[e] The statistically insignificant difference ($p > 0.05$) between the experimental groups and control ABPV. P values were calculated using the Wilcoxon rank sum test.

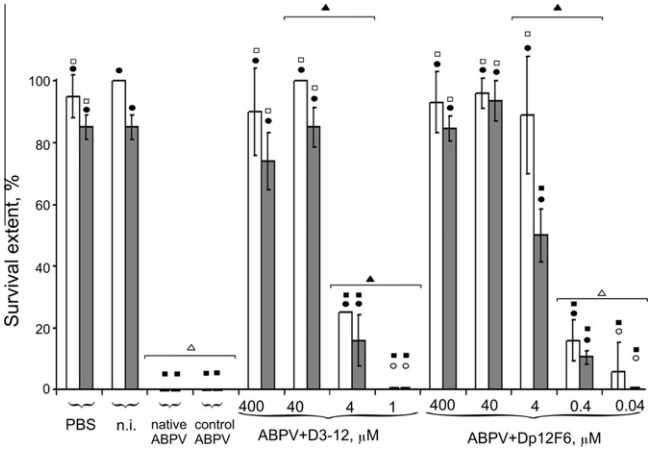

Fig. 3. Survival of bee larvae and adult bees challenged with ABPV pre-treated with aRNases D3–12 and Dp12F6. Groups of ten fourth instar larvae (white bars) or groups of 20 newly emerged adult worker bees (grey bars) were left untreated (n.i.), mock-infected (PBS), infected with native ABPV (10 LD_{50}), infected with ABPV pre-incubated in the absence of aRNase (control ABPV) and ABPV pre-incubated with D3–12 or Dp12F6; p_1 – shows the statistically significant (●, $p1 < 0.01$) or statistically not significant (○, $p_1 > 0.05$) differences between the experimental groups and native ABPV, control ABPV; p_2 – shows the statistically significant (▲, $p_2 < 0.01$) or statistically not significant (△, $p_2 > 0.05$) differences between the experimental groups; p_3 – shows the statistically significant (■, $p_3 < 0.01$) and statistically not significant (□, for $p_3 > 0.05$) differences between the experimental groups and n.i. larvae.

The dependence of larval and bees survival rates on the concentration of aRNases D3–12 and Dp12F6 used for the ABPV inactivation is shown in the Fig. 3. It is seen that pre-treatment of ABPV suspension with aRNase D3–12 within a concentration range from 400 to 40 μM resulted in 90 ± 14.1% to 100% larval survivors. Further decrease of the D3–12 concentration to 4 μM led to a decrease of the survival rate to 25% and at a concentration of 1 μM, the aRNase had no virucidal activity at all. Similar results were obtained for the aRNase Dp12F6, but this compound exhibited a virucidal activity in an even broader range of concentrations (see Fig. 3). Similar dependences were obtained in parallel experiments with adult bees (see grey bars in Fig. 3).

As mentioned above, bee larvae challenged with ABPV display a striking phenotype. We studied the phenotype of bee larvae after injections of aRNase-treated or untreated ABPV, along with the haemolymph proteomic pattern. Pre-incubation of ABPV was carried out in the presence of 0.04–40 μM Dp12F6 followed by injections of 1 μl of this mixture, containing 100 LD_{50} (10 LD_{50} were in Fig. 3) of ABPV, into larvae. Larvae survival rates (Fig. 4A) were equal in the groups injected with 10 and 100 LD_{50} of virus inactivated with 40 μM Dp12F6 confirming the total virus inactivation under these conditions. The injections of 10 LD_{50} of ABPV inactivated with 4 μM Dp12F6 showed 89 ± 19% larval survival, while the injections of 100 LD_{50} of the same preparation resulted in the death of about 40% of larvae. These results indicate that incomplete virus inactivation occurred: the evaluated concentration of still infectious virus was approximately 1 LD_{50}/μl and hence the extent of virus inactivation was 99% (Fig. 4A).

The phenotype of bee larvae injected with ABPV pre-treated with different concentrations of Dp12F6 clearly reflected the measured survival rate. Non-injected and mock-infected larvae 24 h p.i. looked yellowish-white and reached an average weight of 130 mg per larva (Fig. 4B, wells a and b). The larvae challenged with untreated ABPV (10 LD_{50}) did not gain weight 24 h p.i (average

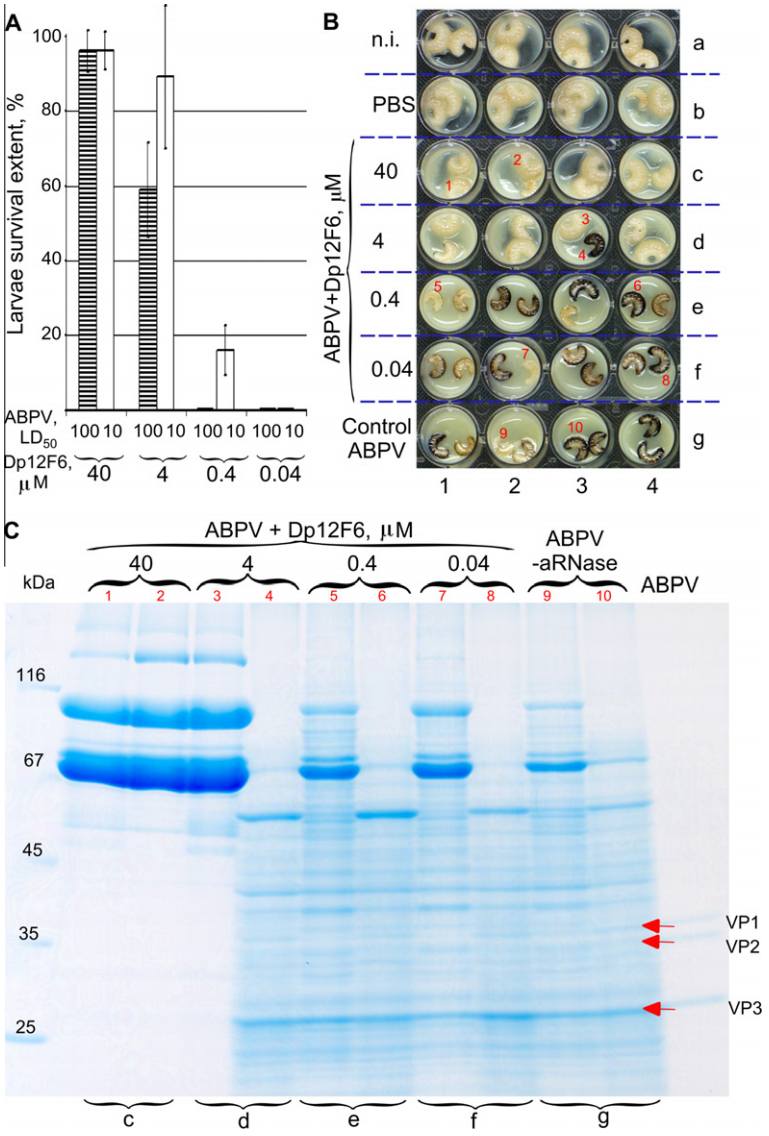

Fig. 4. Phenotypic properties of bee larvae challenged with Dp12F6-treated and untreated ABPV. (A) Survival rate of bee larvae 24 h p.i. of ABPV pre-treated with the indicated concentrations of Dp12F6: aliquots (1 μl) of the incubation mixture were either directly injected into larvae (100 LD_{50}, 10^4 virus particles) – shaded bars or after a 10-fold dilution (10 LD_{50}, 10^3 virus particles) – white bars. (B) Development of the *in vitro* cultured bee larvae injected with ABPV pre-treated with Dp12F6 (concentrations of aRNase are shown on the left). (C) Haemolymph samples were collected from two larvae (indicated by red arabic numbers) out of larvae groups seen in B (wells c to g). Aliquots of these samples were applied onto a 10% polyacrylamide/0.1% SDS gel. At the right, the protein pattern of the purified ABPV suspension utilized in this study is shown, designating three major coat proteins VP1, VP2 and VP3. The red arrowheads point to the newly synthesized viral coat proteins in larvae challenged with ABPV.

weight 60–70 mg) and had turned brownish-dark (Fig. 4B, wells g). The larvae challenged with ABPV pre-treated with Dp12F6 displayed a phenotype that reflects the antiviral effect of Dp12F6 (Fig. 4B): ABPV pre-incubation with 40 μM Dp12F6 and subsequent injection of 100 LD_{50} yielded larvae that looked perfectly healthy (Fig. 4B, wells c). In its turn, injections of 100 LD_{50} of ABPV pre-incubated with 0.04–0.4 μM Dp12F6 provided larvae that expressed all signs of the deadly collapse (Fig. 4B, wells e and f) seen also after injections of the untreated ABPV (Fig. 4B, wells g). Pre-incubation of ABPV suspension with 4 μM Dp12F6 resulted in a differential phenotype: ~60% of larvae developed normally and ~40% did not survive the ABPV infection (Fig. 4B, wells d).

The different response of bee larvae to the challenge with ABPV pre-treated with various concentrations of Dp12F6 can also be seen in the haemolymph protein pattern. Non-infected or PBS-injected bee larvae express a typical class of major proteins (indicated in Fig. 2B) that was still maintained in larvae, which had survived injections of 100 LD_{50} of ABPV suspension pre-treated with 40 μM Dp12F6 (Fig. 4C). This fact indicates that treatment of ABPV with the aRNase averted the infection and virus propagation. On the other hand, protein expression pattern changed dramatically in larvae that had collapsed due to ABPV infection. After the treatment of ABPV with 4 μM Dp12F6 (about 60% larval survival rate, Fig. 4A), two individuals were selected for haemolymph extraction that either have showed no signs of growth retardation (Fig. 4B, larva No. 3) or had collapsed and displayed a brownish colour (Fig. 4B, larva No. 4). A broad spectrum of novel proteins is induced in ABPV-infected larvae along with the accumulation of ABPV virions evident by the production of the three major viral coat proteins VP1, VP2 and VP3 (Fig. 4C, indicated with red arrows). Further decrease of Dp12F6 concentration to 0.4 and 0.04 μM showed the progress of infection, and the protein expression pattern agreed with that in the infected larvae (Fig. 4C).

3.3. The mechanism of virus inactivation

The mechanism of ABPV inactivation was studied in experiments with the Dp12F6 as being the most active aRNase among the compounds tested. We used RT-PCR to confirm the degradation of viral RNA and electron microscopy (EM) to control the morphology of affected virus particles as compared to control ABPV.

3.4. RT-PCR analysis of viral RNA

To confirm that ABPV inactivation by aRNases resulted from the degradation of viral RNA, RT-PCR analysis of viral RNA isolated from aRNase-treated and control virus preparations was performed. To verify the effective isolation of viral RNA and the absence of RNA loss during the isolation steps and RT-PCR analysis, the internal control which is human MDR1 mRNA was added to the virus suspension after its incubation with or without aRNase right before the isolation of viral RNA. Thus, the isolated viral RNA preparations containing both ABPV genomic RNA and MDR1 mRNA were used for RT-PCR analysis.

The location of the amplified fragments of the viral RNA is shown in Fig. 5A. The primer sequences and the sizes of the amplicons are listed in Table 1. Five overlapping fragments of the ABPV genome were chosen: products **1**–**3** correspond to the 5′-part of ORF-1, products **4**–**5** correspond to the 5′-part of ORF-2. The

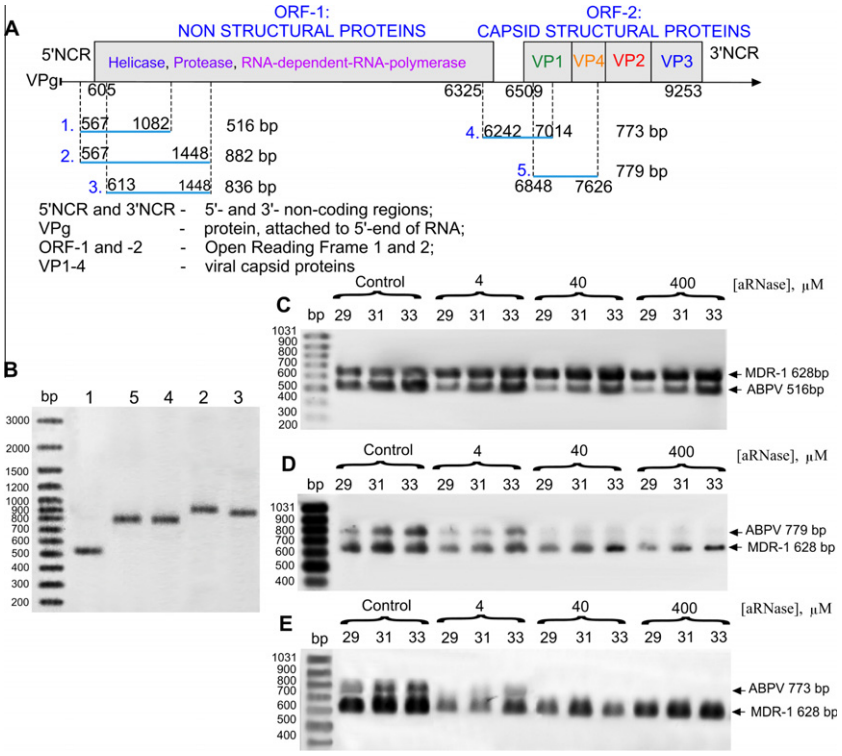

Fig. 5. Analysis of viral RNA isolated from ABPV after inactivation with aRNase Dp12F6. (A) Location of products of ABPV RNA amplification within the structure of the viral genome (according to Govan et al., 2000). Products of RT-PCR obtained with different sets of primer pairs (Table 1) are designated by numbers **1**–**5**. Products **1**–**3** correspond to the 5′-part of ORF-1, encoding non-structural proteins. Products **4** and **5** correspond to the 5′-part of ORF-2, encoding capsid structural proteins. (B) Products of viral RNA amplification obtained with sets of primer pairs **1**–**5**. Digits on top correspond to the utilized primer pairs. (C–E) Results of RT-PCR analysis of viral RNA isolated from aRNase-inactivated and control ABPV. Amplification of MDR1 mRNA was used as internal standard. PCR products were separated in 1% agarose gels and stained with ethidium bromide. ABPV amplification product **1** – in **C**, **4** – **in E** and **5** – in **D**. Digits at the top show the number of cycles of amplification and the concentration of aRNase used to inactivate the virus. As a control, virus suspension was incubated under the conditions of inactivation but in the absence of aRNase. Length of PCR products is shown on the right.

designed primers were selected in order to amplify the overlapping fragments from different regions of ABPV RNA as no certainty exists about the location of possible RNA cleavage sites and absence of data on the structure of viral RNA within the capsid.

Firstly, five fragments **1**–**5** of ABPV genome were amplified (Fig. 5A), showing prominent ABPV-specific products of the expected sizes (Fig. 5B, Table 1). Then MDR-1 mRNA was amplified in the same PCR mixture producing the 628-bp-long PCR product. For simultaneous amplification of viral and MDR-1 RNAs (internal control) three APBV-specific primer sets (**1**, **4** and **5)** were used.

The products of ABPV and MDR-1 amplification are clearly seen for the ABPV preparations incubated in the absence of aRNase (Fig. 5 C–E, lanes "Control"). The exposure of ABPV to aRNase Dp12F6 in the whole range of concentrations led to a decrease of the 516-bp-long ABPV product at 29 cycles of amplification (Fig. 5C, lanes 29 in groups 4, 40 and 400). However, no reliable differences in the intensities of amplification signals at 33 cycles of amplification were observed for Dp12F6-treated and control ABPV (Fig. 5C).

Pre-incubation of ABPV with 40 and 400 μM Dp12F6 resulted in the total disappearance of the 779- and 773-bp-long products (Fig. 5D and E), while these amplification products are present at a reduced level as compared to the control when the virus was incubated with 4 μM Dp12F6. It is worth mentioning that ABPV treated with 40 and 400 μM Dp12F6 corresponded to 96% and 93% larval survival, respectively. Thus, the reduced viral infectivity observed for ABPV treated with Dp12F6 is a result of viral RNA degradation, which prevents ABPV replication. It should be noted that the viral RNA region 6200–7600 nt was cleaved more efficiently than the region 600–1000 nt (primer set **4** and **5** compared to **1**). That could be a result of the packaging of viral RNA within the virus particle or RNA protection by RNA-protein interactions, as well as the influence of RNA secondary and tertiary structure and restrictions imposed on the ability of aRNase to cleave folded RNA fragments.

3.5. Electron microscopic visualization of viral capsids

RT-PCR analysis confirmed that virus inactivation by the aRNase Dp12F6 occurs due to the cleavage of the viral RNA, which could induce alterations in the structure of the inactivated virus particle. To examine these possible alterations we used electron microscopy.

Samples of negatively stained specimens of intact ABPV contain virus particles 20–30 nm in diameter with spherical shape and distinct capsids showing icosahedral symmetry (Fig. 6A). In the control ABPV preparations pre-incubated in the absence of aRNase the virus particles showed a smoother surface and clear-cut center (Fig. 6B). This morphology was observed in all control samples prepared during the experiments. Thus, different patterns of non-damaged ABPV particles are shown in Fig. 6A and B.

The aRNase Dp12F6 was visualized in negatively stained preparations as harsh threads forming aggregates having appearance of a skein of hair, and reaching 1 μm in size (Fig. 6C). Such structures were not found on the grids negatively stained in the absence of aRNase Dp12F6 and on the grids examined in the electron microscope without staining.

To determine the alterations of the structure and morphology of virus particles during the incubation with Dp12F6, the first difficulty to overcome was the sensitivity of the method, which required the elevated concentration of ABPV, as compared to the one used in *in vivo* experiments. Therefore, the increased concentrations of both ABPV and aRNase Dp12F6 were used (see Section 2.11). For these samples the inactivation of virus was proved by RT-PCR: the disappearance of the 779- and 773-bp-long ABPV

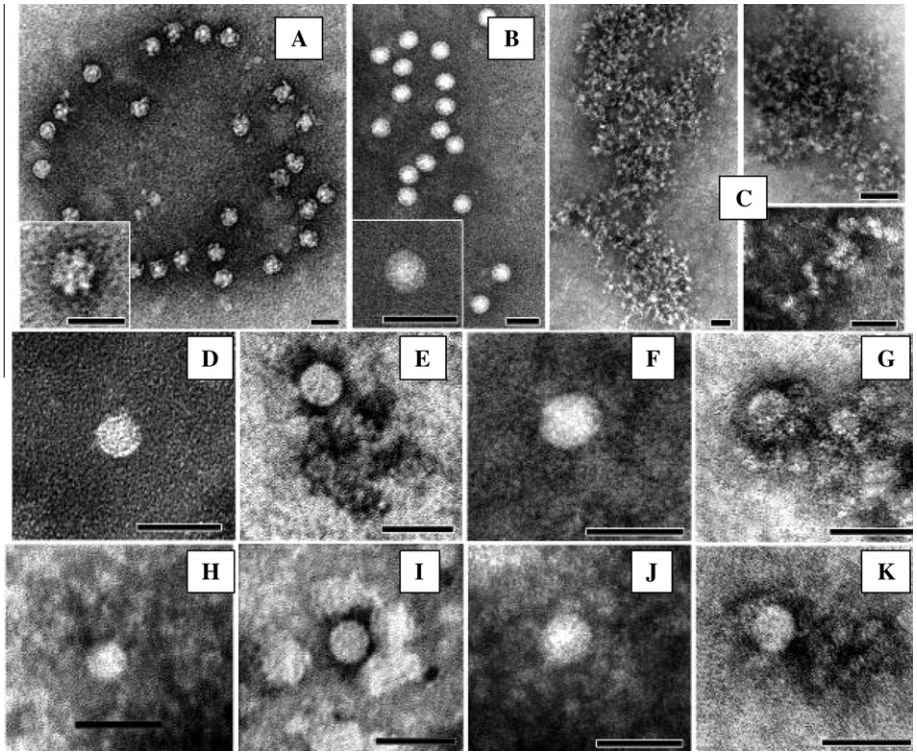

Fig. 6. Transmission electron microscopy of intact ABPV and Dp12F6-inactivated virus preparations. (A and B) Particles of ABPV. A – native virus, B – control virus, incubated under the conditions of inactivation in the absence of aRNase for 24 h. (C). Single thread and aggregations of aRNase Dp12F6 visualized by negative staining with phosphotungstic acid. D–K. The morphology of ABPV particles after the incubation: ABPV particles incubated in the absence (D, F, H and J) and in the presence of Dp12F6 (E, G, I and K) for 5, 8, 12, and 18 h, respectively. Negative staining with phosphotungstic acid. Scale bar 50 nm.

specific products and a slight decrease of the 516-bp-long product (the primary data are not shown).

Examination of ABPV specimens incubated in the presence of aRNase Dp12F6 during 5, 8, 12 and 18 h at 37 °C revealed virus particles tightly associated with the aggregates of aRNase Dp12F6 (Fig. 6E, G, I and K). It should be noted that all ABPV virions in treated preparations looked veiled in contrast to untreated virus (Fig. 6A) and control samples (Fig. 6B). Most probably this "veil" represents gel-like structures which could be formed by the aRNase Dp12F6 in water solutions (Kovalev et al., 2008). However, it was possible to see that the virus particles kept their sizes (diameter 20–30 nm) and spherical shape, no visible damage of the morphology was observed. Thus, the comparison of ABPV morphology in treated and control preparations did not reveal visible differences in the virus structure.

EM was unable to detect signs of virus structure alteration as we have observed previously for enveloped Influenza A virus (Goncharova et al., 2009). This phenomenon may be related to the small size of the ABPV virus particles and their fragments combined with the limited sensitivity of the negative staining method.

Thus we propose that treatment with aRNase Dp12F6 could completely break the virus, and its fragments appear indistinguishable in negatively stained preparations. To verify this suggestion we evaluated the concentration of ABPV particles after incubation with or without Dp12F6 for 0, 8 and 24 h using Latex particles with a known concentration. The concentration of control ABPV after the incubation for 0, 8 and 24 h was around 10^7 particles/ml. The pre-incubation with Dp12F6 for 8 and 24 h resulted in the slight decrease of the virus concentration, which was estimated to be $5–7 \times 10^6$ particles/ml, but this values lie within the experimental error of the method. This fact underlines that no noticeable concentration decrease took place in the Dp12F6-treated samples as compared to control ABPV. The results obtained clearly show that ABPV inactivation and its inability to cause infection in bee larvae are the result of viral RNA cleavage rather than alterations of virus morphology

4. Discussion

Compounds that are able to inactivate viruses and at the same time are low-toxic represent a group of potential therapeutics with respect to both, treatment of the disease and vaccine preparation. In the present study, the ability of artificial ribonucleases to inactivate non-enveloped RNA-viruses was studied using the experimental model bee larvae/ABPV. Previous results showed that aRNases display antiviral activity against enveloped RNA viruses, namely, Influenza A (Goncharova et al., 2009) and tick-borne encephalitis virus (E.P. Goncharova, unpublished results). On the other hand, the ability of aRNases to interact with RNA-protein complexes of non-enveloped viruses, to penetrate into these complexes and to cleave the viral RNA was obscure, as non-enveloped RNA-viruses are characterized by a rigid structure of the virions and stability in the environment (Hendley et al., 1973; Oliveira et al., 1999). Here we demonstrated that aRNases do inactivate the non-enveloped ABPV *via* the destruction of its genomic RNA.

Antiviral activity assessment was performed for five aRNases exhibiting high ribonuclease activity *in vitro*. Two aRNases (Dp12F6 and D3–12) of five compounds tested exhibited a pronounced virucidal effect and one aRNase, i.e. K-D-1, was able to inactivate ABPV, though the experimental error was high possibly due to poor solubility of this aRNase. Two other aRNases L2–3 and ABL3C3 displayed no virucidal activity with respect to ABPV (Table 3). Recently, we have shown that aliphatic fragments present within the structure of aRNases are essential for the high ribonuclease activity of the compounds (Tamkovich et al., 2007). The importance of the hydrophobicity of aRNases is confirmed by the higher virucidal activity of Dp12F6 compared to D3–12: hydrophobocity of fluorine-containing Dp12F6 is much higher compared to D3–12 with hydrogen atoms in the aliphatic fragments (Fig. 1; Rogoza, 1998). The ability of aRNase Dp12F6 to form large supramolecular complexes, similar to those observed for RNA and aRNase Dp12 (Kovalev et al., 2008) was confirmed in the present study by EM (Fig. 6C). Positively charged N-substituted DABCO residues may play a role of a molecular wedge, facilitating the penetration of aRNases into the virion, as it is the first restriction imposed on the compounds intended to interact with viral RNA. The aRNases displaying virucidal activity against ABPV have a total charge of the molecule +4, whereas those which are not active possess the charge +2. Thus, the structure, hydrophobicity and total charge of the aRNase molecule have an impact on the virucidal/antiviral activity of the compounds.

The phenotype of larvae and protein expression pattern in the haemolymph can serve as an indicator of the ABPV infection. The phenotype as well as the protein expression pattern of larvae, which survived after the injection of aRNase-inactivated virus were similar to that of non-injected or mock-injected larvae (Fig. 4B and C). This indicates the total virus inactivation. However, groups of larvae that received injections of ABPV pre-incubated at low concentrations of aRNase showed all signs of ABPV infection (Fig. 4B and C). These data clearly show the sensitivity of bee larvae as a new *in vivo* experimental system to evaluate the extent of virus inactivation by chemical compounds. It should be noted, that honey bees, like all invertebrates, lack an adaptive immune system; instead, they have an efficient "innate immune response", that essentially consists of humoral (i.e., synthesis of antimicrobial peptides) and cellular defense strategies (phagocytosis, encapsulation, nodule formation) to combat bacterial and fungal infections. Recent studies in honey bees (K. Azzami and H. Beier, unpublished results) and in *Drosophila* (Sabatier et al., 2003) suggest that none of these mechanisms are induced after infection with dicistroviruses (ABPV and Drosophila C virus). In other words, we did not observe an "immunoreaction" in ABPV-infected larvae or adult bees that is comparable to bacterial infections (Randolt et al., 2008).

Artificial ribonuclease Dp12F6 inactivates ABPV *via* the cleavage of viral RNA, which was confirmed by RT-PCR (see Fig. 5D and E), and the stability of virion's morphology was proved by EM (see Fig. 6E, G, I and K). The location of the cuts in the genomic RNA of aRNase-treated virus suspension most likely depends on the spatial organization of RNA within the virion: the more exposed the RNA fragment is, the higher is the possibility of its cleavage. Nowadays little is known about the structure and organization of RNA within the capsid of non-enveloped viruses (Davis et al., 2008). The fact, that aRNase Dp12F6 efficiently cleaves the viral RNA at the beginning of ORF-2 (Fig. 5), but leaves the one within the ORF-1 almost intact, provides evidence that the first region is more accessible within the virion. Thus, most likely, it is located either close to the surface of virus particle or/and is less protected by RNA-protein contacts within the virion.

Another factor that can influence the efficiency of RNA cleavage is the presence of Pyr-A motifs located in single-stranded RNA-regions (Zenkova et al., 2001), which are most susceptible to cleavage by aRNases. The cleaved fragment of viral RNA (Fig. 5D) contained 56 C-A and 69 U-A linkages that is 7% and 9%, correspondingly, of the total number of linkages in this 779-nt-long fragment. In turn, the less effectively cleaved 516-nt-long fragment contained 37 C-A and 47 U-A linkages, corresponding also to 7% and 9% of all linkages (Fig. 5C). The equal percentage of Pyr-A motifs in both fragments suggests that not the number of these motifs within the RNA fragment, but the arrangement of the RNA molecule within the virion determined its cleavage potential followed by virus inactivation.

The destruction of viral RNA supports the initially proposed mechanism of the selective virus inactivation by aRNases, which was confirmed by the results of the EM. The EM experiments showed that the titer of virus suspension changes insignificantly after the exposure of ABPV to Dp12F6, as well as the morphology of virus particles does not show any visible differences from the control suspension, being still infectious. The EM analysis of aRNase-inactivated Influenza A virus particles revealed the visible damage of the structure of the virus envelope and breaks of the membrane (Goncharova et al., 2009). These differences could be explained by different mechanisms of aRNase interaction with the virus particles. In the case of Influenza A virus, aRNase ABL3C3 is able to cause membrane distortion prior to RNA cleavage, but leaves the peplomers intact (EM data). In the case of ABPV and Dp12F6 or D3–12, we can speculate that the mechanism of penetration includes interaction either of the aliphatic fragment or the positively charged "head" with the proteins of capsid (neither can be excluded) followed by diffusion of the compound into the virus particles, so that aRNases Dp12F6 and D3–12 act as a molecular wedge leaving no visible signs of interaction.

The advantage of the proposed approach of virus inactivation is that even single cuts within the RNA genome could lead to the inability of virus to propagate. Therefore, this type of inactivated virus particles may represent a new kind of killed-virus vaccine.

For testing of the antiviral activity of aRNases, an experimental model bee larvae/ABPV was developed that permits *in vivo* antiviral activity assessment. This model includes the *in vitro* pre-incubation of ABPV, which is highly pathogenic to honey bees, and its subsequent injection into bee larvae. The antiviral activity can be detected within 24 h and expressed in terms of survival rate and alterations of both the phenotype of larvae and protein expression pattern in the haemolymph of infected individuals. The simplicity of this *in vivo* model is also strengthened by the short period of time needed to perform the screening, which is five days from the collection of larvae until the detection of the antiviral potential of a new compound. Moreover, the simplicity to control a healthy state of the *in vitro* reared larvae (Peng et al, 1992; Randolt et al, 2008), combined with the ethical problems arising when speaking of *in vivo* animal models reveals the reasons of applying the new model. It is worth noting that bee larvae were utilized for numerous studies: screening of the influence of pesticides and other chemicals on larval growth (Peng et al., 1992; Aupinel et al., 2005); the evaluation of the virulence of the bacterial pathogen *Paenibacillus larvae* (Genersch et al., 2005); the humoral immune response of *in vitro* reared bee larvae (Randolt et al., 2008) and others.

Here we reported that artificial ribonucleases are a novel type of antiviral compounds, able to reduce the infectivity of non-enveloped RNA viruses via the cleavage of viral genomic material, while leaving the morphology of the capsid unaltered. We believe that this approach offers a potential for the development of a new type of antivirals and vaccines against RNA viruses. The main benefits of this approach are as follows: degradation of the viral genomic material would abolish the ability of the pathogen to propagate; secondly, the proposed approach is not specifically directed to one type of virus or virus family sharing similarities in structure and biochemistry, but can be applied to a variety of virus species, embracing the group of RNA-containing viruses, in particular, the non-enveloped viruses.

Disclosure statement

All the authors confirm the absence of any actual or potential conflict of interest within publishing the article.

Acknowledgements

This project was financially supported by a grant from the "Deutsche Forschungsgemeinschaft, Sonderforschungsbereich 567" to K. Azzami, H. Beier and J. Tautz; by a grant from Russian Fund for Basic Research No 08-04-01516-a; a grant from Russian Academy of Science program "Molecular and cellular biology". A.A. Fedorova was a recipient of a Leonhard von Euler student fellowship, supported by "Deutscher Akademischer Austauschdienst" (DAAD), Bonn.

References

Aupinel, P., Fortini, D., Dufour, H., Tasei, J.-N., Michaud, B., Odoux, J.-F., Pham-Delègue, M.-H., 2005. Improvement of artificial feeding in a standard *in vitro* method for rearing *Apis mellifera* larvae. Bull. Insectol. 58, 107–111.

Bailey, L., Gibbs, A.J., Woods, R.D., 1963. Two viruses from adult honey bees (*Apis mellifera* Linnaeus). Virology 21, 390–395.

Bakonyi, T., Grabensteiner, E., Kolodziejek, J., Rusvai, M., Topolska, G., Ritter, W., Nowotny, N., 2002. Phylogenetic analysis of Acute bee paralysis virus strains. Appl. Environ. Microbiol. 68, 6446–6450.

Ball, B.V., 1985. Acute bee paralysis virus isolates from honeybee colonies infested with *Varroa jacobsoni*. J. Apic. Res. 24, 115–119.

Broo, K., Wei, J., Marshall, D., Brown, F., Smith, T.J., Johnson, J.E., Schneemann, A., Siuzdak, G., 2001. Viral capsid mobility: a dynamic conduit for inactivation. Proc. Natl. Acad. Sci. USA 98, 2274–2277.

Davis, M., Sagan, S.M., Pezacki, J.P., Evans, D.J., Simmonds, P., 2008. Bioinformatic and physical characterizations of genome-scale ordered RNA structure in mammalian RNA viruses. J. Virol. 82, 11824–11836.

Genersch, E., Ashiralieva, A., Fries, I., 2005. Strain- and genotype-specific differences in virulence of *Paenibacillus larvae* subsp. *larvae*, a bacterial pathogen causing American foulbrood disease in honeybees. Appl. Environ. Microbiol. 71, 7551–7555.

Genersch, E., Aubert, M., 2010. Emerging and re-emerging viruses of the honey bee (*Apis mellifera* L.). Vet. Res. 41, 54.

Goncharova, E.P., Kovpak, M.P., Ryabchikova, E.I., Konevets, D.A., Sil'nikov, V.N., Zenkova, M.A., Vlassov, V.V., 2009. Viral genome cleavage with artificial ribonucleases: a new method to inactivate RNA-containing viruses. Dokl. Biochem. Biophys. 427, 221–224.

Govan, V.A., Leat, N., Allsopp, M., Davison, S., 2000. Analysis of the complete genome sequence of Acute bee paralysis virus shows that it belongs to the novel group of insect-infecting RNA viruses. Virology 277, 457–463.

Hendley, J.O., Wenzel, R.P., Gwaltney Jr., J.M., 1973. Transmission of rhinovirus colds by self-inoculation. N. Engl. J. Med. 288, 1361–1364.

Konevets, D.A., Beck, I.E., Beloglazova, N.G., Sulimenkov, I.V., Sil'nikov, V.N., Zenkova, M.A., Shishkin, G.V., Vlassov, V.V., 1999. Artificial ribonucleases: synthesis and RNA cleaving properties of cationic conjugates bearing imidazole residues. Tetrahedron 55, 503–512.

Kostenko, E.V., Laktionov, P.P., Vlassov, V.V., Zenkova, M.A., 2002. Downregulation of PGY/MDR1 mRNA level in human KB cells by antisense oligonucleotide conjugates. RNA accessibility in vitro and intracellular antisense activity. Biochim. Biophys. Acta 1576, 143–147.

Kovalev, N., Burakova, E., Silnikov, V., Zenkova, M., Vlassov, V., 2006. Artificial ribonucleases: from combinatorial libraries to efficient catalysts of RNA cleavage. Bioorg. Chem. 34, 274–286.

Kovalev, N.A., Medvedeva, D.A., Zenkova, M.A., Vlassov, V.V., 2008. Cleavage of RNA by an amphiphylic compound lacking traditional catalytic groups. Bioorg. Chem. 36, 33–45.

Kuznetsova, I., Silnikov, V.N., 2004. Small ribonuclease mimics. In: Zenkova, M.A. (Ed.), Artificial Nucleases. Springer-Verlag, Berlin, Heidelberg, pp. 111–128.

Kuznetsova, I.L., Zenkova, M.A., Gross, H.J., Vlassov, V.V., 2005. Enhanced RNA cleavage within bulge-loops by an artificial ribonuclease. Nucleic Acids Res. 33, 1201–1212.

Laemmli, U.K., 1970. Cleavage of structural proteins during the assembly of the head of bacteriophage T4. Nature 227, 680–685.

Mittereder, N., March, K.L., Trapnell, B.C., 1996. Evaluation of the concentration and bioactivity of adenovirus vectors for gene therapy. J. Virol. 70, 7498–7509.

Newman, J.F.E., Brown, F., Bailey, L., Gibbs, A.J., 1973. Some physico-chemical properties of two honey-bee picornaviruses. J. Gen. Virol. 19, 405–409.

Oliveira, A.C., Ishimaru, D., Gonçalves, R.B., Smith, T.J., Mason, P., Sá-Carvalho, D., Silva, J.L., 1999. Low temperature and pressure stability of picornaviruses: implications for virus uncoating. Biophys. J. 76, 1270–1279.

Peng, Y.-S.C., Mussen, E., Fong, A., Montague, M.A., Tyler, T., 1992. Effects of chlortetracycline of honey bee worker larvae reared *in vitro*. J. Invertebr. Pathol. 60, 127–133.

Randolt, K., Gimple, O., Geissendörfer, J., Reinders, J., Prusko, C., Mueller, M.J., Albert, S., Tautz, J., Beier, H., 2008. Immune-related proteins induced in the hemolymph after aseptic and septic injury differ in honey bee worker larvae and adults. Arch. Insect Biochem. Physiol. 69, 155–167.

Rogoza, A.V., 1998. Superlipophilicity (xenophilicity) and microlipophilicity of perfluorinated saturated groups. Part 1. Qualitative selection criteria for biologically active substances containing perfluorinated fragments,

International Conference on Natural Products and Physiologically Active Substances (ICNPAS-98), November 30–December 6, 1998, Novosibirsk, Russia.
Sabatier, L., Jouanguy, E., Dostert, C., Zachary, D., Dimarcq, J.-L., Bulet, P., Imler, J.-L., 2003. Pherokine-2 and -3. Two *Drosophila* molecules related to pheromone/odor-binding proteins induced by viral and bacterial infections. Eur. J. Biochem. 270, 3398–3407.
Singer, B., Fraenkel-Conrat, H., 1969. Chemical modification of viral ribonucleic acid. VIII. The chemical and biological effects of methylating agents and nitrosoguanidine on tobacco mosaic virus. Biochemistry 8, 3266–3269.
Tate, J., Liljas, L., Scotti, P., Christian, P., Lin, T., Johnson, J.E., 1999. The crystal structure of cricket paralysis virus: the first view of a new virus family. Nat. Struct. Biol. 6, 765–774.
Tamkovich, N.V., Malyshev, A.V., Konevets, D.A., Sil'nikov, V.N., Zenkova, M.A., Vlassov, V.V., 2007. Chemical ribonucleases: VII. Effect of positively charged RNA-binding domains and hydrophobic fragments of the conjugates based on 1, 4-diazabicyclo[2.2.2]octane and imidazol on their ribonuclease activity. Bioorg. Khim. 33, 251–260.
Tamkovich, N.V., Zenkov, A.N., Vlassov, V.V., Zenkova, M.A., 2010. An RNA sequence determines the speed of its splitting by artificial ribonucleases. Bioorg. Khim. 36, 223–235.
Zenkova, M., Beloglazova, N., Sil'nikov, V., Vlassov, V., Giegé, R., 2001. RNA cleavage by 1,4-diazabicyclo[2.2.2]octane-imidazole conjugates. Methods Enzymol. 341, 468–490.